AD-A118 586   SRI INTERNATIONAL   MENLO PARK CA   F/G 20/8
               THEORETICAL STUDY OF STATE-TO-STATE COLLISIONS.(U)
               JUN 82   C H BECKER, R P SAXON, A P HICKMAN   F49620-80-C-0064
UNCLASSIFIED   SRI-MP-82-063   AFOSR-TR-82-0668   NL

END
DATE
FILMED
9 82
DTIC

AFOSR-TR- 82-0668

⑤

June 29, 1982

Final Scientific Report
Covering the Period 1 May 1980 to 30 April 1982

THEORETICAL STUDY OF STATE-TO-STATE COLLISIONS

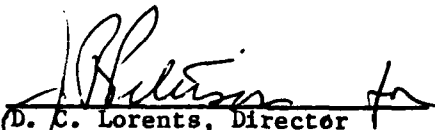By: Christopher H. Becker, Roberta P. Saxon, and
Albert P. Hickman

Prepared for:

AIR FORCE OFFICE OF SCIENTIFIC RESEARCH
Bolling Air Force Base
Washington, DC 20332

Attention: Dr. Ralph Kelley

Approved:

D. C. Lorents, Director
Molecular Physics Laboratory

G. R. Abrahamson, Vice President
Physical Sciences Division

REPORT DOCUMENTATION PAGE	READ INSTRUCTIONS BEFORE COMPLETING FORM

1. REPORT NUMBER AFOSR-TR- 82-0668	2. GOVT ACCESSION NO. AD - A118585	3. RECIPIENT'S CATALOG NUMBER

4. TITLE (and Subtitle) Theoretical Study of State-to-State Collisions	5. TYPE OF REPORT & PERIOD COVERED Final Scientific Report 1 May 1980 - 30 April 1982
	6. PERFORMING ORG. REPORT NUMBER MP 82-063

7. AUTHOR(s) Christopher H. Becker, Roberta P. Saxon, and Albert P. Hickman	8. CONTRACT OR GRANT NUMBER(s) F49620-80-C-0064

9. PERFORMING ORGANIZATION NAME AND ADDRESS SRI International 333 Ravenswood Avenue Menlo Park, California 94025	10. PROGRAM ELEMENT, PROJECT, TASK AREA & WORK UNIT NUMBERS 61102F 2301/A4

11. CONTROLLING OFFICE NAME AND ADDRESS Air Force Office of Scientific Research Bolling Air Force Base Washington, DC 20332	12. REPORT DATE June 1982
	13. NUMBER OF PAGES 39

14. MONITORING AGENCY NAME & ADDRESS(If different from Controlling Office)	15. SECURITY CLASS. (of this report) Unclassified
	15a. DECLASSIFICATION/DOWNGRADING SCHEDULE

16. DISTRIBUTION STATEMENT (of this Report)

Distribution unlimited

17. DISTRIBUTION STATEMENT (of the abstract entered in Block 20, if different from Report)

18. SUPPLEMENTARY NOTES

19. KEY WORDS (Continue on reverse side if necessary and identify by block number)

triatomic collisions, Rydberg atom collisions, nonadiabatic collisions, ion pair formation, symmetric charge exchange

20. ABSTRACT (Continue on reverse side if necessary and identify by block number)

The probability of making transitions between specifically known molecular states in collisional processes has been investigated theoretically. Fully quantum mechanical close-coupled calculations of electronic-vibrational-translational energy exchange for model atom-diatomic potentials have been performed. The process of ion-pair formation was investigated in this work.

DD FORM 1473 EDITION OF 1 NOV 65 IS OBSOLETE

Block 20. (continued)

Symmetric charge exchange in diatomic ion-diatomic molecule collisions was also studied. Nonadiabatic collisions were studied by quasi-classical and quantum perturbation methods as well. Finally, scaling laws for collisions of atomic Rydberg states with atoms and molecules have been developed.

Accession For

NTIS GRA&I

DTIC TAB

Unannounced

Justification

By

Distribution/

Availability Codes

Avail and/or

Dist   Special

A

DTIC COPY INSPECTED 2

CONTENTS

I INTRODUCTION

The objectives of this project are to develop the theoretical tools necessary to treat a variety of molecular state-to-state collision processes and to perform calculations of transition probabilities for selected systems. The problems considered here have involved the interactions of three particles under the influence of potentials for two or more electronic states. For this type of process, currently available experimental techniques allow the determination of specific states of species before and after interaction. Our general approach has been to pursue two types of calculations: model calculations designed to isolate and probe particular reaction mechanisms, and calculations focused on specific systems that have been studied experimentally in our laboratory or elsewhere. This dual approach has enabled us to better understand a wide range of scattering phenomena and has provided a quantitative test of the accuracy of the methods we have developed and of frequently used approximations.

During the past year we have devoted the major part of our effort to detailed time-independent quantum mechanical calculations of ion pair formation and related vibrational excitation processes in atom-diatomic collisions. We also are applying the methods developed in this work to the case of symmetric molecular charge exchange. In related work, we have treated the process of ion-pair formation in nonadiabatic collisions by quasi-classical trajectory surface hopping and quantum mechanical perturbation theory techniques. Finally, previous rigorous coupled channel calculations of cross sections for ℓ-mixing of Na Rydberg states in collisions with atoms and molecules have been complemented by the development of a simple scaling law for these cross sections. All of these accomplishments are described briefly in the following section.

II RESEARCH ACCOMPLISHMENTS

Coupled-Channel Calculations of Vibrational Excitation and Ion-Pair Formation: K + O_2

A significant fraction of our effort under this program has been devoted to the investigation of electronic-vibrational-translational energy exchange in nonadiabatic collisions. Fully quantum mechanical coupled channel scattering calculations were performed on a model potential surface designed to model the system

$$K + O_2(v_i) \rightarrow K + O_2(v_f)$$
$$\rightarrow K^+ + O_2^-(v_f) \tag{1}$$
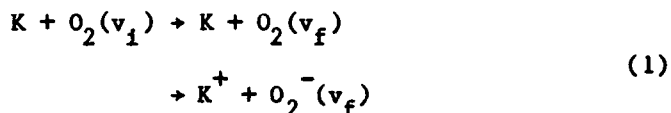
This system is an attractive candidate for theoretical study because experimental data are available at different collision energies by different workers,[1,2] and data from this laboratory[3] are also available for the related Ar* + O_2 system. The latter results showed the interesting effect of mediation of the vibrational distribution in the initial channel by the presence of the ion-pair channel. Since the present quantum calculations are essentially dynamically exact, they will serve as a benchmark for other computational approaches. They also help elucidate the dynamics of the efficient flow of energy between different vibrational levels in the presence of nonadiabatic coupling. Finally, in the course of making these calculations, we have improved the state-of-the-art methodology for streamlining large scale scattering calculations.

In these calculations, only the doublet potential surfaces arising from the $K(^2S) + O_2(^3\Sigma_g^-)$ ground state asymptote and the $K^+(^1S) + O_2^-(^2\Pi_g)$ ion pair asymptote were considered. Simplified but realistic interaction potentials were taken from a classical collision model fit to data.[2] The interaction was taken to be isotropic (no rotational excitation) to make the problem more tractable and to focus on the vibronic aspects of the problem. Coulomb boundary conditions for the ion-pair formation channels had to be incorporated

explicitly. The collision energies studied were over the broad range 0.27, 0.68, 12.5, and 43.5 eV. Predominantly a basis set was used consisting of 16 neutral and 16 ionic vibrational eigenfunctions. Extensive testing of convergence with number of vibrational channels was performed.

The results of the calculations show that vibrational energy transfer is efficient in nonadiabatic collisions, typically being a significant fraction of the gas-kinetic cross section. At the two highest energies, the integral cross sections (Q) for scattering from $K + O_2(v = 0)$ for ion-pair formation are very roughly governed by the $O_2-O_2^-$ Franck-Condon factors for the transitions. The neutral pair Q's show a slow monotonic fall-off with v. At low energies, the Q's are dominated by energy availability. The effect of O_2^- vibration can be seen in the opacity functions and differential cross sections that were calculated quantum mechanically, and the effect can be related to the collision time and the O_2^- vibrational period in a classical surface-hopping model. The structure in the high energy loss peaks of neutral products from TOF measurements[1] is rather well reproduced in these calculations. This suggests that much of this inelasticity is due to ground electronic state vibrational excitation.

A paper on this work, published in the Journal of Chemical Physics, gives the theoretical methods and results in detail. (See list of papers in Section III and abstract in Appendix A).

Symmetric Molecular Charge Exchange

As a further probe of efficient vibrational energy exchange in nonadiabatic collisions, we have also completed a study of symmetric molecular scattering in the ground electronic state system

$$O_2^+(v_i) + O_2(v_i') \rightarrow O_2^+(v_f) + O_2(v_f')$$

$$\rightarrow O_2(v_f') + O_2^+(v_f) \qquad (2)$$
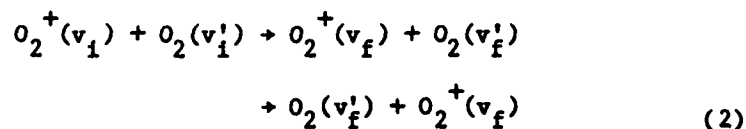
The direct and charge transfer (exchange) scattering characteristic of symmetric systems leads to much larger vibrationally inelastic and momentum transfer cross sections than for asymmetric systems.

One previous theoretical formulation for this problem exists, given by Bates and Reid.[4] It approximates the treatment of translational motion by using a classical trajectory. Also, to make the problem more tractable, the rotational degree of freedom was ignored. This formulation[4] is a form of the so-called impact parameter approximation of scattering theory.[5] This method is frequently applied at hyperthermal and even thermal energies, often without due consideration of its accuracy. It is known from general considerations that the approximation improves at higher energies, and it is usually considered valid for most cases around 10 eV.[5]

A completely quantum mechanical formulation for symmetric molecular scattering has, to our knowledge, been lacking until now. It appeared worthwhile to examine the reliability of the impact parameter approximation (using different classical trajectories) by comparing with fully quantum mechanical coupled-channel scattering calculations. Therefore, we formulated the problem and performed the coupled-channel calculations at center-of-mass collision energies of 1, 8, and 36 eV.

A unitary transformation was found to reduce the 2n coupled radial equations to two sets of n coupled equations. This reduction in dimensionality significantly reduces the computational labor because the computing time scales approximately as the cube of the number of coupled equations.

The coupled radial Schrödinger equations were numerically integrated by the log-derivative algorithm developed by Johnson.[6,7] Convergence was checked for integration step size, integration range, and number of channels needed in the basis set. It was found that basis size convergence was more difficult at 1 eV than at 8 or 36 eV. A somewhat similar result was found in the $K + O_2$ coupled channel calculations.

The impact parameter method of Bates and Reid[4] has been applied by Moran and coworkers[8-10] to the $O_2^+-O_2$ system, using both straight line and effective curved trajectories. Comparison of the relative probabilities for transitions at a particular impact parameter for 1 eV collisions from the present calculations with the straight line and curved trajectory classical path calculations of Ref. 10 show essentially no agreement between any of the three methods. Comparison of integral cross sections shows that agreement is not particularly

close between any of the approaches at 8 eV and is qualitative only at 36 eV. It is expected that, as the energy increases, the classical path approximation will be increasingly accurate.

A paper on this subject is to be published in the <u>Journal of Chemical Physics</u> (see Appendix B and list of publications in Section III).

Model Calculations of Nonadiabatic Collisions

Under this program we have also completed studies of atom-molecule collisions that involve two or more electronic potential energy surfaces using both quasi-classical and quantum mechanical perturbation techniques, as described below.

Quasi-Classical Surface Hopping Model

This model invokes the Landau-Zener formula to calculate a surface-hopping probability at each surface intersection. Using the surface-hopping model, we performed a comparative study of ion-pair formation on two similar systems:

$$Ar^* + I_2 \rightarrow Ar^+ + I_2^- \tag{3}$$

and

$$K + I_2 \rightarrow K^+ + I_2^- \tag{4}$$

One would expect these two reactions to be rather similar, because in each case the single active electron is in a 4s orbital. However, an additional final channel is available in the first reaction. Penning ionization may occur,

$$Ar^* + I_2 \rightarrow Ar + I_2^+ + e^- \tag{5}$$
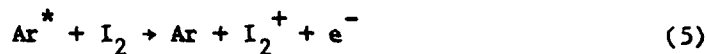
Data are available for both ion-pair reactions.[11,12,13] We were able to perform calculations that explained some of the differences in the differential cross sections for these two systems. We explored how differences in the

matrix elements arising from the inner-shell vacancy and the competing ionization channel would affect the cross sections. A paper on this work has been published in the _Journal of Chemical Physics_ (see list of papers in Section III and abstract in Appendix A).

Quantum Mechanical Perturbation Theory of Nonadiabatic Collisions

In this work, we sought an alternative to the coupled-channel quantum mechanical formulation of nonadiabatic collisions that would preserve the essential features of the multiple-surface crossings, but exploited approximations that can legitimately be made at high collision energies ($E \sim 50-100$ eV). The approach chosen was the impact parameter approximation, in which a rectilinear classical trajectory is assumed for the translational motion, leading to a time-dependent Schrödinger's equation for the remaining degrees of freedom. We discovered that model potentials of the same type used in previous studies of collisions of alkali atoms and diatomic molecules led to a particularly simple form of the final equations. These equations were solved using the Magnus approximation.

We will summarize the results of our calculations. We performed calculations using model potentials chosen to model the reaction

$$Cs + O_2 \rightarrow Cs^+ + O_2^- \tag{6}$$

Initially, isotropic potentials were assumed; that is, molecular rotation was neglected. The results exhibited strong oscillations, corresponding qualitatively to those observed in recent measurements.[14] These oscillations have been related to the vibrational motion of the molecular potentials using the infinite-order-sudden approximation. We obtained rotationally averaged cross sections between specific vibrational states. The oscillations observed in the isotropic case persisted, although they were less prominent.

These rotationally averaged calculations also enabled us to examine the effect of different initial vibrational levels v_i on the ion-pair formation. The model predicted that the oscillations will become less pronounced as v_i is increased. Although no measurements are available to test this result, our calculations suggest a direction for future experiments.

The theory and calculations are described in a paper that has been published by the Journal of Chemical Physics (see Section III and Appendix A).

Theoretical Studies of Rydberg Atoms

During the past year, we have completed a study of physical scaling laws for the angular momentum mixing of Na Rydberg states in collisions with atoms and molecules. We have found that the results of many coupled-channel and Born calculations can be expressed in terms of numerically determined functions of reduced parameters. The general result is

$$\sigma_{\ell-mix}(n) = \pi n^4 a_o^2 g(\beta) f(\gamma) \tag{7}$$

where $\sigma_{\ell-mix}(n)$ is the experimentally measured ℓ-mixing cross section summed over all final states ℓ'; β is a quantity that measures the strength of the interaction of the collision partner with the diffuse electron cloud; and γ is a quantity related to the energy gap between the nd and higher nℓ states of Na. The functions of g and f are not analytic but have been calculated and make simple graphs. This equation thus leads to an interpretation of the scattering process in terms of reduced parameters that have a clear physical meaning.

The formula has been applied to collisions of Na(nd) with He, Ne, Ar, N_2, CH_4, C_3H_8; to Rb(nf) + He, Ar, Xe; and to Xe(nf) + CO_2. The results are generally accurate to about a factor of two. This degree of accuracy is very useful because the cross sections vary by an order of magnitude or more in the range of n considered. A paper on this work has been published in Physical Review A (see Section III and Appendix A).

III PUBLICATIONS UNDER THIS PROGRAM

A. C. H. Becker and R. P. Saxon, "A Coupled-Channel Study of Electronic-Vibrational-Translation Energy Exchange in Nonadiabatic Collisions," J. Chem. Phys. $\underline{75}$, 4899 (1981).

B. C. H. Becker, "Quantum Mechanical Calculations of Symmetric Molecular Charge Exchange and Vibrational Excitations in $O_2^+ + O_2$ Collisions," to be published in J. Chem. Phys.

C. A. P. Hickman and K. T. Gillen, "Comparison of Ion-Pair Formation in the Systems $Ar^* + I_2$ and $K + I_2$," J. Chem. Phys. $\underline{73}$, 3672 (1980).

D. A. P. Hickman, "Model for Fast Non-Adiabatic Collisions Between Alkali Atoms and Diatomic Molecules," J. Chem. Phys. $\underline{73}$, 4413 (1980).

E. A. P. Hickman, "Approximate Scaling Formula for Collisional Angular-Momentum Mixing of Rydberg Atoms," Phys. Rev. A $\underline{23}$, 87 (1981).

REFERENCES

1. C. E. Young, C. M. Scholeen, A. F. Wagner, A. E. Proctor, L. G. Pobo, and S. Wexler, J. Chem. Phys. 74, 1770 (1981).

2. (a) A. W. Kleyn, V. N. Khromov, and J. Los, Chem. Phys. 52, 65 (1980);
   (b) A. W. Kleyn, E. A. Gislason, and J. Los, Chem. Phys. 52, 81 (1980).

3. K. T. Gillen and T. M. Miller, Phys. Rev. Lett. 45, 624 (1980).

4. D. R. Bates and R.H.G. Reid, Proc. Roy. Soc. A 310, 1 (1969).

5. See, e.g., S. Geltman, Topics in Atomic Collision Theory (Academic Press, New York, 1969).

6. B. R. Johnson, J. Comp. Phys. 13, 445 (1973).

7. B. R. Johnson, Chem. Phys. 2, 381 (1973).

8. T. F. Moran, M. R. Flannery, and P. C. Cosby, J. Chem. Phys. 61, 1261 (1974).

9. T. F. Moran, K. J. McCann, and M. R. Flannery, J. Chem. Phys. 63, 3857 (1975).

10. T. F. Moran, K. J. McCann, M. Cobb, R. F. Borkman, and M. R. Flannery, J. Chem. Phys. 74, 2325 (1981).

11. J. A. Aten, G.E.H. Lanting, and J. Los, Chem. Phys. 19, 241 (1977).

12. J. A. Aten and J. A. Los, Chem. Phys. 25, 47 (1977).

13. K. T. Gillen, T. D. Gaily, and D. C. Lorents, Chem. Phys. Lett. 57, 192 (1978).

14. A. W. Kleyn, M. M. Hubers, and J. Los. Chem. Phys. 34, 55 (1978).

APPENDIX A

ABSTRACTS OF PUBLICATIONS

A coupled-channel study of electronic–vibrational–translational energy exchange in nonadiabatic collisions

C. H. Becker and R. P. Saxon

Molecular Physics Laboratory, SRI International, Menlo Park, California 94025

Fully quantum mechanical coupled-channel calculations of electronically nonadiabatic collisions in the presence of many vibrational states have been performed over a range of collision energies from 0.27 to 43.5 eV. The calculations were based on simplified model potentials for $K + O_2$, considering the doublet potential curves arising from the ground electronic neutral $K(^2S) + O_2(^3\Sigma_g^-)$ and ionic $K^+(^1S) + O_2^-(^2\Pi_g)$ states, and assuming isotropic interaction. Comparison of calculated scattering properties and recent experimental results at hyperthermal energies for $K + O_2$ indicates that the simplified model interaction nevertheless gives a good physical description. This work investigates the collision dynamics, while providing a reference for other more approximate theoretical approches. Processes leading to neutral and ionic products are discussed for this system where many vibronic channels are strongly coupled.

J. Chem. Phys. <u>75</u>, 4899 (1981).

Comparison of ion pair formation in the systems $Ar^* + I_2$ and $K + I_2$

A. P. Hickman and Keith T. Gillen

Molecular Physics Laboratory, SRI International, Menlo Park, California 94025

A simple model that has been used extensively by Los and co-workers to treat ion pair formation in collisions of alkali atoms with diatomic molecules is extended to include continuum coupling via a competing Penning ionization channel. This extended model is then used to calculate the differential cross sections for ion pair formation for the system $Ar^* + I_2$ over the energy range 28–154 eV and to compare with a previous treatment of $K + I_2$. In the absence of significant competition from continuum processes, Ar^* is expected to behave in a manner similar to K, since the active electron is an unpaired $4s$ electron in both cases. We perform model calculations for $Ar^* + I_2$ to investigate the effects of varying the potential curves and charge exchange matrix elements and of including a continuum coupling function $\Gamma(R)$. Comparison with previous calculations for $K + I_2$ suggests increased repulsion on the Ar^*-I_2 surfaces relative to those of $K-I_2$. The competing mechanisms of excitation transfer and Penning ionization may have a small effect upon the ion pair angular distributions.

J. Chem. Phys. <u>73</u>, 3672 (1980).

Model for fast, nonadiabatic collisions between alkali atoms and diatomic molecules

A. P. Hickman

Molecular Physics Laboratory, SRI International, Menlo Park, California 94025

Equations for collisions involving two potential surfaces are presented in the impact parameter approximation. In this approximation, a rectilinear classical trajectory is assumed for the translational motion, leading to a time-dependent Schroedinger's equation for the remaining degrees of freedom. Model potentials are considered for collisions of alkali atoms with diatomic molecules that lead to a particularly simple form of the final equations. Using the Magnus approximation, these equations are solved for parameters chosen to model the process $Cs + O_2 \rightarrow Cs^+ + O_2^-$, and total cross sections for ion-pair formation are obtained as a function of energy. The results exhibit oscillations that correspond qualitatively to those seen in recent measurements. In addition, the model predicts that the oscillations will become less pronounced as the initial vibrational level of O_2 is increased.

J. Chem. Phys. <u>73</u>, 4413 (1980).

Approximate scaling formula for collisional angular-momentum mixing of Rydberg atoms

A. P. Hickman

Molecular Physics Laboratory, SRI International, Menlo Park, California 94025

An approximate scaling formula has been determined that permits the rapid estimation of cross sections for angular-momentum-changing collisions of Rydberg atoms with a variety of targets, using information about low-energy-electron scattering from the target. The formula is obtained by fitting the results of coupled-channel and Born-approximation calculations to functions of reduced parameters. Application to $Na(nd)$ + He, Ne, Ar, N_2, CH_4, C_2H_6; $Rb(nf)$ + He, Ar, Xe; and $Xe(nf)$ + CO_2, suggests that the accuracy is about a factor of 2.

QUANTUM MECHANICAL CALCULATIONS OF SYMMETRIC MOLECULAR CHARGE EXCHANGE AND VIBRATIONAL EXCITATIONS IN $O_2^+ + O_2$ COLLISIONS

C. H. Becker
Molecular Physics Laboratory
SRI International
Menlo Park, California 94025

ABSTRACT

A scattering formulation is presented for symmetric molecular charge exchange treating the internal vibrational degrees of freedom and translation quantum mechanically. A unitary transformation is found to reduce the 2n coupled radial equations to two sets of n coupled equations. The formulation is applied to $O_2^+(X^2\Pi_g, v) + O_2(X^3\Sigma_g^-, v')$ at 1, 8, and 36 eV center-of-mass collision energies. Convergence with respect to vibrational basis set size is found to be slower at lower energy. Integral cross sections and transition probabilities as a function of nuclear orbital angular momentum are presented. The integral cross sections summed over final levels for vibrational excitation and deexcitation and for charge transfer are on the order of 10 Å^2. Comparisons of earlier classical path calculations with the present results do not show quantitative agreement at these energies.

I. INTRODUCTION

Symmetric atomic and molecular charge transfer are important in the behavior of ionized gases. While a great deal has been learned about symmetric atomic charge transfer,[1] comparatively little work has been done on symmetric molecular charge transfer. In the molecular case, the exchange of vibrational-translational energy as well as electron exchange may be quite efficient.

The first work that explicitly included the vibrational degrees of freedom for molecular charge exchange was by Bates and Reid.[2] This was a classical path (also known as impact parameter) type scattering approximation using a time-dependent framework. The translational motion is treated classically and the internal degrees of freedom are treated quantum mechanically. This treatment is expected to be reliable in the 100-1000 eV collision energy range. The approximation surely degrades at some point below this, but it is unclear where.

Recently, Moran et al.[3] performed calculations studying $O_2^+ + O_2$ collisions between 0.5 and 8 eV kinetic energy with the formulation of Ref. 2. Comparison was made between a straight-line trajectory and an effective curved trajectory for the classical path. It is reasonable to expect that, for lower energies, a curved trajectory approach would give a better description.

This paper presents a formulation for the symmetric molecular charge exchange process that treats all degrees of freedom quantum mechanically. A unitary transformation is then found to reduce the dimensionality of the problem. The formulation is then applied to $O_2^+ + O_2$ collisions and the results are compared with classical path calculations.[3-5]

A quantum mechanical coupled-channel formulation is used to describe the symmetric molecular charge exchange scattering. We assume that the symmetric scattering is rotationally elastic, as assumed in the earlier treatment of Bates and Reid.[2] Therefore, the rotational eigenfunctions are dropped from the basis set, though they could be included in a straight-forward manner. Rotational excitation could in principle be treated exactly or treated within some approximate framework if anisotropic potentials are known.[6]

Consider two molecules, labeled A and B, with vibrational coordinates r_a and r_b, and the distance of separation of the centers-of-mass of the two molecules given by R. In theory, we can distinguish two ground state electronic configurations: when molecule A is $O_2^+(X^2\Pi_g, v)$ and molecule B is $O_2(X^3\Sigma_g^-, v')$, the "direct," or D, electronic state results, and when molecule A is $O_2(X^2\Sigma^-, v')$ and B is $O_2^+(X^2\Pi_g, v)$ the "exchange," or X, electronic state results. Higher electronic states of O_2^+ and O_2 are ignored; this should not have a significant effect at the investigated collision energies.

The total wavefunction is taken as the diabatic expansion

$$\Psi(r_a, r_b, R, \rho) = \psi^D(\rho) \sum_v \phi_v(r_a) \chi_{v'}(r_b) F_v^D(R)$$

$$+ \psi^X(\rho) \sum_v \phi_v(r_b) \chi_{v'}(r_a) F_v^X(R)$$

(1)

where $\psi^{D,X}(\rho)$ are the diabatic electronic eigenfunctions of the electronic coordinates ρ, and $\phi_v(r)$ and $\chi_{v'}(r)$ are vibrational eigenfunctions for O_2^+ and O_2, respectively.

Combinations of O_2^+ and O_2 vibrational levels are denoted by $\nu \equiv (v, v')$, and $F_\nu^{D,X}(R)$ are the radial wavefunctions for each channel containing the scattering information (at large R).

The total Hamiltonian is written

$$H = H_{el} + T(R) + T(r_a) + T(r_b) \tag{2}$$

where H_{el} is the Hamiltonian for the electronic degrees of freedom, and T is the kinetic energy operator. The projection of H_{el} on the electronic eigenfunctions yields

$$H_{el}\psi^D = U^D(R)\psi^D + [V_+(r_a) + V_0(r_b)]\psi^D \tag{3a}$$

$$H_{el}\psi^X = U^X(R)\psi^X + [V_0(r_a) + V_+(r_b)]\psi^X . \tag{3b}$$

Here $U^{D,X}$ represents the intermolecular interaction, and V_0, V_+ are the neutral and ionic diatomic potential functions.

Substituting Eqs. (1, 2, and 3) into the time-independent nonrelativistic Schrödinger equation, multiplying on the left by $(\psi^D)^*$, or $(\psi^X)^*$, and integrating over ρ yields

$$\left[V^D(R) + T(R) + T(r_a) + V_{+,0}(r_a) + T(r_b) + V_{0,+}(r_b) - E\right]$$

$$\times \sum_\nu \phi_v(r_{a,b})\chi_{v'}(r_{b,a})F_\nu^{D,X}(R) +$$

$$\tag{4}$$

$$\left[V^X(R) + \zeta\left(T(R) + T(r_a) + V_{0,+}(r_a) + T(r_b) + V_{+,0}(r_b) - E\right)\right]$$

$$\times \sum_\nu \phi_v(r_{b,a})\chi_{v'}(r_{a,b}) F_\nu^{X,D}(R) = 0$$

where

$$\zeta = \langle\phi^D|\phi^X\rangle = \langle\phi^X|\phi^D\rangle, \quad V^X(R) \equiv \langle\phi^D|U^X(\rho, R)|\phi^X\rangle_\rho = \langle\phi^X|U^D(\rho, R)|\phi^D\rangle_\rho,$$

$$V^D(R) \equiv \langle\phi^D|U^D(\rho, R)|\phi^D\rangle_\rho = \langle\phi^X|U^X(\rho, R)|\phi^X\rangle_\rho, \text{ and Eq. (4) implies the two}$$

equations corresponding to the first or second sub- or superscripts.   In
writing Eq. (4) we have neglected the nonadiabatic coupling of the nuclear
kinetic energy operators acting on the electronic wavefunctions, that is we
have invoked a Born-Oppenheimer approximation.

Noting the vibrational Schrödinger equations

$$\left(T(r_{a,b}) + V_+(r_{a,b})\right)\phi_v(r_{a,b}) = \epsilon_v\phi_v(r_{a,b}) \text{ and}$$

$$\left(T(r_{a,b}) + V_0(r_{a,b})\right)\chi_{v'}(r_{a,b}) = \epsilon_{v'}\chi_{v'}(r_{a,b}), \quad \text{writing } \epsilon_\nu = \epsilon_v + \epsilon_{v'},$$

using the indices ν and μ, and closing on Eq. (4) with $\langle\phi_v(r_a)|\langle\chi_{v'}(r_b)|$
yields

$$\left[T(R) + V^D(R) + \epsilon_\mu - E\right]F^D_\mu(R)$$

$$+ \sum_\nu\left[V^X(R) + \zeta(T(R) + \epsilon_\nu - E)\right]P_{\mu\nu}F^X_\nu(R) = 0 \tag{5}$$

and

$$\left[V^X(R) + \zeta(T(R) + \epsilon_\mu - E)\right]F^D_\mu(R)$$

$$+ \sum_\nu\left[V^D(R) + T(R) + \epsilon_\nu - E\right]P_{\mu\nu}F^X_\nu(R) = 0 \tag{6}$$

where $P_{\mu\nu} = P_{\nu\mu} = p(v_\mu, v'_\nu)p(v_\nu, v'_\mu)$ in which $p(v, v') = \langle\phi_v(r)|\chi_{v'}(r)\rangle$
is a vibrational overlap integral.

Rewriting Eq. (6) as

$$\sum_\nu\left[T(R) + \epsilon_\nu - E\right]P_{\mu\nu}F^X_\nu(R)$$

$$= - \sum_\nu V^D(R)P_{\mu\nu}F^X_\nu(R) - \left[V^X(R) + \zeta(T(R) + \epsilon_\mu - E)\right]F^D_\mu(R) \tag{7}$$

and substituting Eq. (7) into Eq. (5) and rearranging yields

$$\{(1 - \zeta^2)[T(R) + \varepsilon_\mu + V^D(R) - E] - \zeta[V^X(R) - \zeta V^D(R)]\}F^D_\mu(R)$$

$$+ \sum_\nu [V^X(R) - \zeta V^D(R)]P_{\mu\nu}F^X_\nu(R) = 0. \qquad (8)$$

For symmetric systems, we use the relationship[7,8]

$$(1 - \zeta^2)\bar{V} = V^X - \zeta V^D \qquad (9)$$

where $\bar{V}(R)$ is the governing intermolecular interaction (to be discussed shortly). Using Eq. (9), Eq. (8) is rewritten as

$$[T(R) + \varepsilon_\mu + V^D(R) - \zeta\bar{V}(R) - E]F^D_\mu(R) = - \sum_\nu \bar{V}(R)P_{\mu\nu}F^X_\nu(R) . \qquad (10)$$

Analogously, one finds

$$[T(R) + \varepsilon_\mu + V^D(R) - \zeta\bar{V}(R) - E]F^X_\mu(R) = - \sum_\nu \bar{V}(R)P_{\mu\nu}F^D_\nu(R) . \qquad (11)$$

For n combinations of v and v', Eqs. (10) and (11) constitute a set of 2n coupled equations—n direct and n exchange channels.

For numerical solution of Eqs. (10) and (11) a simple partial wave expansion[9] is taken for $F^{D,X}(R)$,

$$F^{D,X}_\mu(R) = \sum_\ell \frac{i^\ell(2\ell + 1)}{k_\mu R} P_\ell(\cos \theta)f^{\ell,(D,X)}_\mu(R) \qquad (12)$$

B-6

where P_ℓ is the Legendre polynomial, and θ is the scattering angle. More precisely, one should consider the nuclear statistics.[9] For ^{16}O, the nuclear spin is zero, Bose-Einstein statistics govern, and the expansion Eq. (12) should be written with the summation $2 \sum\limits_{\ell(\text{even})} \ldots$. For large numbers of partial waves, as in the present application, little error is incurred in the integral cross sections using Eq. (12). The set of equations of the form of Eqs. (10) and (11) can then be written, now in matrix form, as

$$\left[\underset{\sim}{I} \frac{d^2}{dR^2} + \underset{\sim}{k}^2 - \underset{\sim}{I} \frac{\ell(\ell + 1)}{R^2} - \underset{\sim}{W}(R) \right] \underset{\sim}{f}^\ell(R) = 0 \quad . \tag{13}$$

This is a matrix equation of 2n dimension. Matrix elements are indexed by μ and ν and by D and X. Here $\underset{\sim}{I}$ is the unit matrix, ℓ is the nuclear orbital angular momentum, $\underset{\sim}{k}^2$ is a diagonal matrix with elements $k^2_{\substack{\mu\nu \\ DX}} = \frac{2\mu}{\hbar^2} (E - \varepsilon_\mu) \delta_{\mu,\nu} \delta_{D,X}$, and $\underset{\sim}{W}(R)$ is a symmetric matrix with elements

$$W_{\substack{\mu\nu \\ DX}}(R) = \frac{2\mu}{\hbar^2} \left\{ (1 - \delta_{D,X}) P_{\mu\nu} \overline{V}(R) + \delta_{\mu,\nu} \delta_{D,X} \left[V^D(R) - \zeta \overline{V}(R) \right] \right\} . \tag{14}$$

The radial wavefunctions are given by the 2n dimensional square matrix $\underset{\sim}{f}^\ell(R)$; each column is a linear independent solution to the scattering problem corresponding to a different initial channel.

The matrix of regular solutions $\underset{\sim}{f}^\ell(R)$ can be written as

$$\underset{\sim}{f} = \underset{\sim}{u}^- - \underset{\sim}{u}^+ \underset{\sim}{k}^{-1/2} \underset{\sim}{S} \underset{\sim}{k}^{1/2} \tag{15}$$

where $\underset{\sim}{u}^\pm$ are diagonal with the elements being the Ricatti-Hankel functions at large R,[10] and approaching $\exp\left[\pm i \left(k_{\mu\mu} R - \frac{\ell\pi}{2} \right) \right]$ as $R \to \infty$. Also $\underset{\sim}{f}(0) = 0$. The $\underset{\sim}{k}^{\pm 1/2}$ are diagonal with elements $k^{\pm 1/2}$ dropping the

subscripts, and at large R $\underset{\sim}{S}$ is the symmetric and unitary scattering matrix. The transition matrix is given by $\underset{\sim}{T} = \underset{\sim}{I} - \underset{\sim}{S}$.

Using Eq. (15), the matrix equation (13) can be written schematically in D and X blocks as

$$\begin{pmatrix} \underset{\sim}{a} & \underset{\sim}{b} \\ \underset{\sim}{b} & \underset{\sim}{a} \end{pmatrix} \left\{ \begin{pmatrix} \underset{\sim}{u}^- & 0 \\ 0 & \underset{\sim}{u}^- \end{pmatrix} - \begin{pmatrix} \underset{\sim}{u}^+ & 0 \\ 0 & \underset{\sim}{u}^+ \end{pmatrix} \begin{pmatrix} \underset{\sim}{k}^{-1/2} & 0 \\ 0 & \underset{\sim}{k}^{-1/2} \end{pmatrix} \begin{pmatrix} \underset{\sim}{S}_{DD} & \underset{\sim}{S}_{DX} \\ \underset{\sim}{S}_{XD} & \underset{\sim}{S}_{XX} \end{pmatrix} \begin{pmatrix} \underset{\sim}{k}^{1/2} & 0 \\ 0 & \underset{\sim}{k}^{1/2} \end{pmatrix} \right\} = 0 \quad (16)$$

Here $\underset{\sim}{a}$, $\underset{\sim}{u}^{\pm}$, and $\underset{\sim}{k}^{\pm 1/2}$ are n-dimensional diagonal matrices, $\underset{\sim}{a}$ has

elements $\dfrac{d^2}{dR^2} + k^2_{\mu\mu} - \dfrac{\ell(\ell+1)}{R^2} - \dfrac{2\mu}{\hbar^2} \left[V^D(R) - \zeta \bar{V}(R) \right]$, $\underset{\sim}{b}$ has symmetric

elements $\dfrac{-2\mu}{\hbar^2} P_{\mu\nu} \bar{V}(R)$, $\underset{\sim}{S}_{DX} = \underset{\sim}{S}_{XD} \equiv \underset{\sim}{S}_X$, and $\underset{\sim}{S}_{DD} = \underset{\sim}{S}_{XX} \equiv \underset{\sim}{S}_D$.

The symmetry of the system can be used to reduce the problem from 2n dimensions to two problems each of n dimensions. As the computing time for numerical solution of these equations generally scales as the total number of channels cubed, this can make an important difference. Also computer storage problems are diminished. The unitary matrix which diagonalizes Eq. (16) is found to be a general rotation matrix, written in block form as

$$\begin{pmatrix} \cos(\pi/4)\underset{\sim}{I} & \sin(\pi/4)\underset{\sim}{I} \\ -\sin(\pi/4)\underset{\sim}{I} & \cos(\pi/4)\underset{\sim}{I} \end{pmatrix} = \frac{1}{\sqrt{2}} \begin{pmatrix} \underset{\sim}{I} & \underset{\sim}{I} \\ -\underset{\sim}{I} & \underset{\sim}{I} \end{pmatrix} \equiv \underset{\sim}{Z} \quad (17)$$

Multiplying Eq. (16) on the left by $\underset{\sim}{Z}^t$ (the t signifies transpose) and on the right by $\underset{\sim}{Z}$ leads to a block diagonal form. The two blocks are the matix equations

$$(\underset{\sim}{a} \pm \underset{\sim}{b})\{\underset{\sim}{u}^- - \underset{\sim}{u}^+ \underset{\sim}{k}^{-1/2}(\underset{\sim}{S}_D \pm \underset{\sim}{S}_X) \underset{\sim}{k}^{1/2}\} = 0 \quad . \quad (18)$$

By integrating Eq. (18) to large R, for both signs, the $\underset{\sim}{S}_D$ and $\underset{\sim}{S}_X$ then can be constructed.

In analogy to atom-atom charge (or excitation) transfer,[1] the plus solution of Eq. (18) corresponds to gerade (g) state scattering while the minus solution corresponds to ungerade (u) state scattering. The $\underset{\sim}{S}_D$ and $\underset{\sim}{S}_X$ matrices are reconstructed from the g and u solutions.

The interaction potential $\overline{V}(R)$ is taken as one-half the gerade-ungerade eigenvalue splitting.[8] The identification of $\overline{V}(R)$ from Eq. (9) as one-half the g-u splitting is based on a molecular analogy to the equivalence between the two atom LCAO approximation for $2\overline{V}(R)$ and the g-u splitting, neglecting the electron exchange and electron motion between atoms.[8] For these calculations the isotropic $\overline{V}(R)$ is taken from Ref. 4.

The diagonal potential term $V^D - \zeta\overline{V}$ is found from the Morse and Sato function evaluation[4] of the gerade and ungerade eigenvalues

$$\varepsilon_g = (V^D - \zeta\overline{V}) + \overline{V} = D_e\left\{\exp\left[-2\beta(R-R_e)\right]-2\exp\left[-\beta(R-R_e)\right]\right\} \tag{19a}$$

$$\varepsilon_u = (V^D - \zeta\overline{V}) - \overline{V} = \frac{1}{2} D_e\left\{\exp\left[-2\beta(R-R_e)\right]+2\exp\left[-\beta(R-R_e)\right]\right\} \tag{19b}$$

From Eq. (19) we find

$$V^D - \zeta\overline{V} = D_e\left\{(3/4)\exp\left[-2\beta(R-R_e)\right] -(1/2)\exp\left[-\beta(R-R_e)\right]\right\} . \tag{20}$$

Due to the Sato approximation for ε_u, there is an unphysical crossing of ε_g and ε_u at $R^*(=4.306$ bohr for the parameters used[4]). For values of $R<R^*$, $V^D-\zeta\overline{V}$ is taken to be ε_g, and $\overline{V}$ is taken to be zero.

III. RESULTS AND DISCUSSION

Numerical integration of the coupled equations (Eqs. (18)) was performed for $O_2^+ + O_2$ by the log-derivative integration algorithm of Johnson.[11] For the computations at 8 and 36 eV, where all channels of the basis set are energetically open, the integration was performed out to a distance beyond all classical turning points where a connection was made to a multichannel JWKB propagation[12] (see also Ref. 13). By propagating the multichannel JWKB solution over small steps using the repeated Magnus approximation,[12] the S-matrix elements from the JWKB solution converged to the S-matrix elements from the fully integrated equations, at least within the working accuracy of the integration which is $|S_{\mu\nu}|^2$ values accurate to within 0.001. (The log-derivative integration and JWKB propagation step sizes and end points were chosen to maintain an accuracy in $|S_{\mu\nu}|^2$ of 0.001 for a given basis set.) The effects of different basis set sizes on the results will be discussed shortly.

The products of overlap integrals were calculated by direct numerical integration of Morse function vibrational wavefunctions. The Morse parameters were taken from Ref. 14 for $O_2^+(X^2\Pi_g)$ and $O_2(X^3\Sigma_g^-)$. With regard to comparisons to the scattering results of Moran et al.,[3-5] the overlap integral products used in this work do not differ from the values derived from RKR potentials reported in Ref. 4 by more than about 0.001. This difference is expected to be unimportant in comparisons between the different scattering computational approaches.

Calculations at 1 eV

In constructing the basis set, the number of channels was incremented according to the maximum number of vibrational quanta in the $O_2^+ + O_2$ system. For example, for a maximum of 2 quanta, the number of channels in the basis set (ignoring presently D versus X in the channel count), is n = 6 corresponding to the combinations $v = (v, v') = (0,0), (0,1), (1,0), (0,2), (1,1), (2,0)$. For 3 quanta n = 10, for 11 quanta n = 78, i.e., n is the binomial coefficient $\binom{y+2}{2}$ where y is the maximum number of quanta.

Scattering calculations at 1 eV collision energy relative to $O_2^+(v = 1) + O_2(v' = 0)$ were performed at only one value of orbital angular momentum ($\ell = 92$, corresponding to an impact parameter b = 2.00 bohr) because it was found that the number of channels required to achieve well converged results precluded calculations over many values of ℓ. A study of the vibrational basis set convergence properties at 1 eV collision energy for the initial channel (1,0) is presented in Table 1. Values of the square modulus of the D and X S-matrix elements are presented. Phase convergence of the S-matrix elements follow a similar trend. The slowest channels to converge are, as expected, the elastic D and X channels, while the energetically closest channel (0,1) ($\Delta E \simeq 320$ cm^{-1}) is second-slowest to converge. The slowness of the elastic channel convergence probably reflects the sensitivity of the charge transfer process to modest changes in scattering phase accumulation with the addition of more coupled channels. As can be seen in Table 1, about 78 channels are required to achieve agreement between consecutive basis sets to about 1% for the elastic D and X probabilities.

A comparison of the relative probabilities for the transitions from (1,0) for b = 2.00 bohr and 1 eV by the present calculations (Table 1) with the straight line and curved trajectory classical path calculations of Ref. 3 show essentially no agreement between any of the three methods.

Calculations at 8 eV

Channel convergence tests for the (1,0) channel for kinetic energy of 8 eV relative to $O_2^+(v = 1) + O_2(v' = 0)$ were performed up to n = 45 channels (ignoring D versus X in the channel count) for ℓ = 136 and 816. It was found that n = 21 channels at ℓ = 136 gave convergence of $\left| S_{\mu,\nu}^{D,X} \right|^2$ for the slowest converging elastic channels to within about 4%, and within 1% for inelastic channels, which was deemed sufficient to carry out the calculation over a grid of ℓ-waves (impact parameters). Better convergence was found for ℓ = 816. The spacing used was $\Delta\ell$ = 34 corresponding to Δb = 0.26 bohr. The larger number of channels needed at the lower collision energy perhaps is indicative of more phase accumulation or more vibrationally adiabatic behavior. At both 1 and 8 eV the O_2^+, O_2 molecules have enough time during the collision for more than one vibrational period. Thus classical vibrational timing arguments[13] do not seem capable of explaining the convergence difference.

The relative transition probabilities as a function of ℓ or b are seen plotted in Figs. 1 and 2 in a manner that allows direct comparison to the straight-line and effective curved trajectory calculations of Ref. 3. Comparison with the two classical path approximations shows that agreement with the fully quantal calculations is at best only qualitative for this system at 8eV.

Absolute transition probabilities for the scattering at 8 eV out of (1,0) are shown as a function of ℓ for the major inelastic direct channels in Fig. 3 and inelastic exchange channels in Fig. 4. The elastic exchange probabilities are plotted in Fig. 5. Some interesting similarities appear between several D and X proabilities in Figs. 3 and 4, but a sound explanation for the detailed

form of the transitions is not apparent at this time. Note that the

$(1,0) \rightarrow (0,1)$ transition probability extends in ℓ considerably beyond the

other inelastic channels leading to larger integral cross sections, as

expected. Inelastic transitions as a function of ℓ involving the

(de)excitation of one or more total quanta show a maximum and a falloff at

$\ell \simeq 500$, which corresponds to a classical turning point around R^*, the ε_g

and ε_u crossing at 4.3 bohr. That the critical classical turning point is

around R^* (this is also found at 36 eV), and not greater than or equal to the

maximum in $\overline{V}$ (5.0 bohr), suggests that a large $d\overline{V}/dR$ is important in

producing more highly inelastic transitions, because for R just greated than

R^* the $d\overline{V}/dR$ is largest. The form of $d\overline{V}/dR$ near the ε_g and ε_u crossing is

strongly model dependent. It is noted that the cross sections for

$(1,0) \rightarrow (1,0)$ and $(0,1)$ are less sensitive to this region of ε_g, ε_u crossing.

Values of some integral cross sections at 8 eV from $O_2^+(v = 1)$

$+ O_2(v = 0)$ are given in Table 2 together with some comparisons to classical

path calculations.[3] Spline interpolated values of $|T^\ell|^2$ are used in the

present results, so the values are approximate but should be reliable to

within a few per cent as the figures indicate. The figures also indicate that

the chosen spacing in $\Delta\ell$ gives an accurate description of the collision

because of the smoothness of the probabilities as a function of ℓ. The

results of Table 2 and comparison of Figs. 1 and 2 with those of Ref. 3 do not

indicate that the curved trajectory is a significant improvement over a

straight-line trajectory. Agreement is not particularly close between any of

the three approaches at 8 eV.

Calculations at 36 eV

Channel convergence tests for scattering at 36 eV center-of-mass colli-
sion energy relative to the (0,0) channel showed that the basis set conver-
gence was more rapid than at 8 eV. A total of n = 21 channels were used in
the coupled-channel calculations with a grid of ℓ waves using $\Delta\ell$ = 68
corresponding to Δb = 0.25 bohr. Absolute transition probabilities as a
function of ℓ for scattering from (1,0) are shown for the elastic charge
exchange process in Fig. 5, for the inelastic direct channels in Fig. 6, and
for the inelastic charge exchange channels in Fig. 7. Comparison of the 8 and
36 eV elastic charge exchange probabilities (Fig. 5) shows significant
similarities; the main differences are that transitions occur out to slightly
larger impact parameters at lower energy and that the 8 eV results show
additional strong oscillations (phase interference), both suggesting the
importance of more phase accumulation at lower energy.

Total, i.e., summed over final states, inelastic and total charge
exchange integral cross sections Q at 36 eV from the present results and those
from straight-line trajectory calculations of Refs. 4 and 5 are compared in
Table 3. As can be seen, agreement is qualitative only. Similar agreement is
found for state-to-state integral cross sections. It is expected that as the
energy increases, the classical path approximation will be increasingly
accurate.

Charge-exchange and vibrationally inelastic cross sections have been
found to be rather large, as seen in Tables 2 and 3 indicating rapid energy
migration in ionized oxygen, and large momentum transfer cross sections.

In summary, a quantum mechanical coupled-channel formulation has been
presented for symmetric molecular charge exchange. A unitary transformation
was found to reduce the set of 2n coupled radial equations to two sets of n

coupled equations. Calculations have been applied to the $O_2^+ + O_2$ system at 1, 8, and 36 eV center-of-mass collision energies. Vibrational basis set size convergence is very slow at 1 eV, but becomes more rapid at 8 eV, and more rapid still at 36 eV. Comparisons of classical path scattering approximation calculations with the present calculations, which treat translation quantum mechanically, show substantial quantitative disagreement for the $O_2^+ + O_2$ system at these energies. Better agreement between coupled-channel and classical path calculations would be expected at higher collision energies.
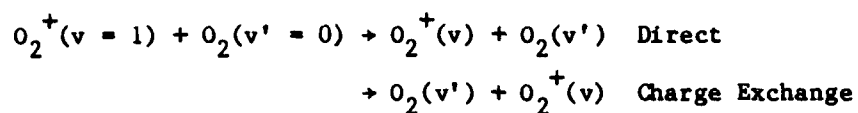
Acknowledgement

REFERENCES

1. See, for example, N. F. Mott and H.S.W. Massey, _The Theory of Atomic Collisions_ (Oxford, 1965); and H.S.W. Massey, E.H.S. Burhop, and H. B. Gilbody, _Electronic and Ionic Impact Phenomena_, 2nd edition (Oxford, 1971), Vol. III.

2. D. R. Bates and R.H.G. Reid, Proc. Roy. Soc. A 310, 1 (1969).

3. T. F. Moran, K. J. McCann, M. Cobb, R. F. Borkman, and M. R. Flannery, J. Chem. Phys. 74, 2325 (1981).

4. T. F. Moran, M. R. Flannery, and P. C. Cosby, J. Chem. Phys. 61, 1261 (1974).

5. T. F. Moran, K. J. McCann, and M. R. Flannery, J. Chem. Phys. 63, 3857 (1975).

6. Regarding the rotational elasticity approximation, a recent experiment on $N_2^+ + N_2$ collisions at 800 eV has shown no observable rotational excitation for charge exchanged N_2^+, but modest excitation for the direct channel. See, K. Richter and A. Ding, Proc. of European Conf. of Atomic Physics, Heidelberg, 1981, p. 678.

7. E. F. Gurnee and J. L. Magee, J. Chem. Phys. 26, 1237 (1957).

8. M. R. Flannery, P. C. Cosby, and T. F. Moran, J. Chem. Phys. 59, 5494 (1973).

9. E.H.S. Burhop in _Quantum Theory_, editor D. R. Bates (Academic, New York, 1961), Vol. I, Ch. 9.

10. F. Calogero, _Variable Phase Approach to Potential Scattering_ (Academic, New York 1967), Appendix I.

11. B. R. Johnson, J. Comp. Phys. 13, 445 (1973).

12. B. R. Johnson, Chem. Phys. 2, 381 (1973).

13.   C. H. Becker and R. P. Saxon, J. Chem. Phys. 75, 4899 (1981).

14.   P. H. Krupenie, J. Phys. Chem. Ref. Data 1, 423 (1972).

Table 1.   Values of the square modulus of direct and exchange S-matrix elements for selected final channels, μ, from the $\nu = (1,0)$ channel at 1 eV collision energy for $\ell = 92$ as a function of the number of vibrational channels in the basis set, n.

μ	$|S^D_{\mu\nu}|^2$	$|S^X_{\mu\nu}|^2$	$|S^D_{\mu\nu}|^2$	$|S^X_{\mu\nu}|^2$
	n = 15		n = 21	
0,0	0.00012	0.00007	0.00010	0.00006
0,1	0.0081	0.0930	0.0127	0.0861
1,0	0.1801	0.7175	0.1312	0.7685
0,2	0.00080	0.00009	0.00076	0.00007
	n = 28		n = 36	
0,0	0.00009	0.00005	0.00009	0.00004
0,1	0.0174	0.0690	0.0207	0.0558
1,0	0.1679	0.7442	0.2307	0.6914
0,2	0.00075	0.00006	0.00072	0.00005
	n = 45		n = 55	
0,0	0.00008	0.00003	0.00008	0.00003
0,1	0.0223	0.0478	0.0228	0.0435
1,0	0.2886	0.6400	0.3288	0.6035
0,2	0.00071	0.00005	0.00070	0.00005
	n = 66		n = 78	
0,0	0.00008	0.00003	0.00008	0.00003
0,1	0.0229	0.0414	0.0229	0.0404
1,0	0.3513	0.5830	0.3629	0.5724
0,2	0.00069	0.00005	0.00069	0.00005

Table 2 Integral cross sections $Q(\text{Å}^2)$ at 8 eV for

$$O_2^+(v = 1) + O_2(v' = 0) \rightarrow O_2^+(v) + O_2(v') \quad \text{Direct}$$

$$\rightarrow O_2(v') + O_2^+(v) \quad \text{Charge Exchange}$$

Final Channel (v, v')	Q^D	Q^X
0,0	0.11,[a] 0.66,[b] 0.76[c]	0.14,[a] 0.37,[b] 0.38[c]
0,1	2.23, 1.75, 1.79	1.80, 1.72, 2.41
1,0	73.95	26.40
0,2	0.90, 0.55, 0.64	1.16, 0.98, 0.20
1,1	1.05, 0.83, 0.87	1.23, 0.93, 1.52
2,0	0.03, 0.48, 0.70	0.05, 0.78, 0.85
0,3	0.07, 0.07	0.04, 0.05
1,2	0.02	0.10
2,1	0.02	0.02
3,0	0.01	0.01

[a] The first column is the present results.

[b] The second column is the straight-line trajectory results of Ref. 3.

[c] The third column is the curved trajectory results of Ref. 3.

Table 3 Integral cross section $Q(\text{Å}^2)$ at 36 eV for

$$O_2^+(v) + O_2(v') \to O_2^+(v) + O_2(v') \quad \text{Direct}$$

$$\to O_2(v') + O_2^+(v) \quad \text{Charge Exchange}$$
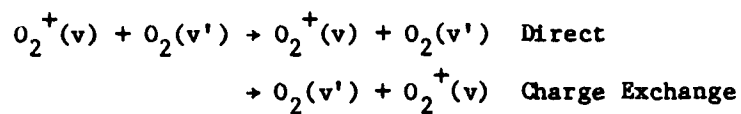
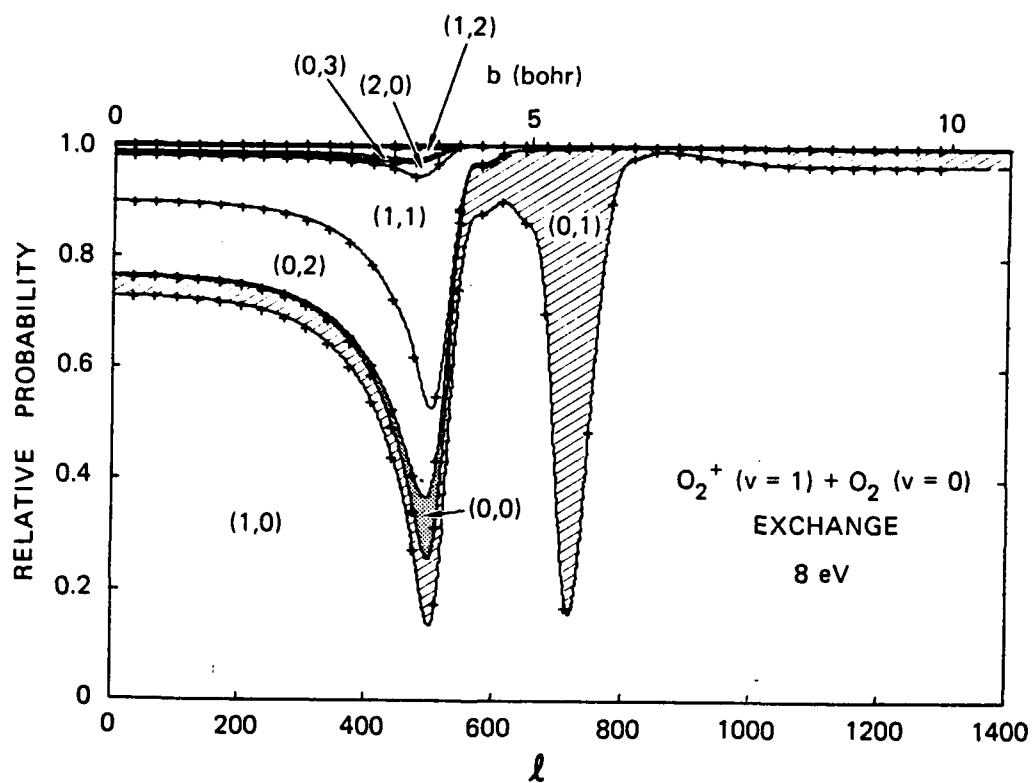| Initial Channel (v, v')	Total Inelastic Q	Total Charge Exchange Q
0,0	5.5,[a] 2.7[b]	16.4,[a] 29.[b]
1,0	13.6, 7.1	29.5, c
2,0	19.4, 11.1	23.2, 31.

[a]First column is from the present fully quantum mechanical coupled-channel results.

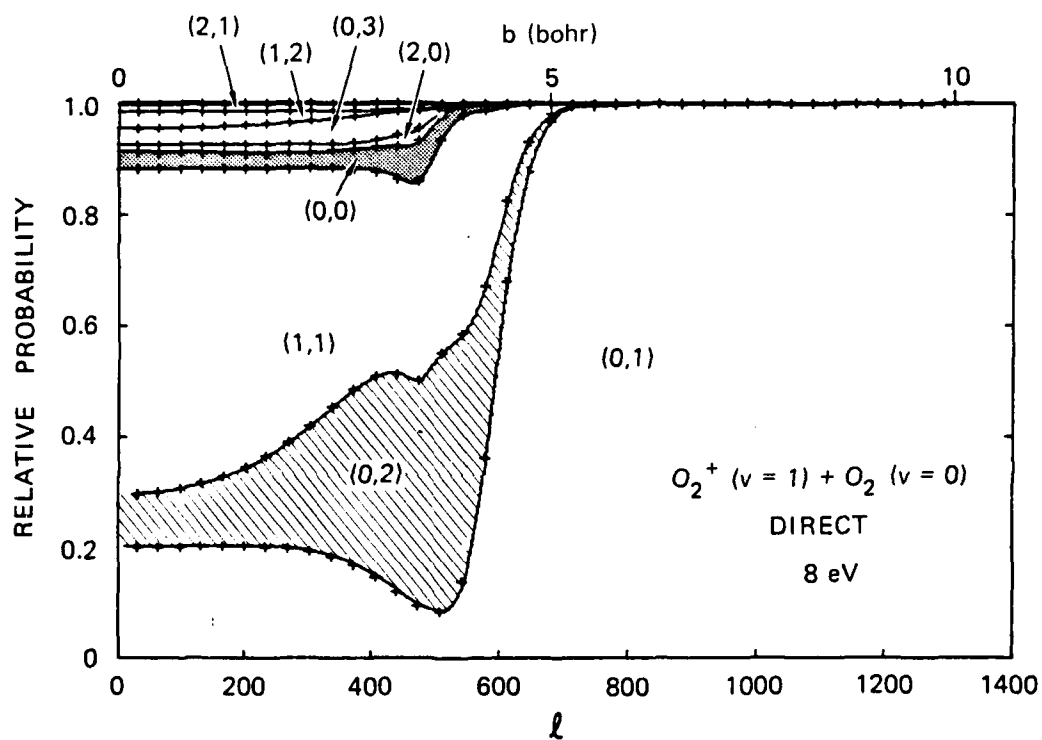[b]Second column is from straight-line classical path calculations of Refs. 4 and 5.

[c]Not available.

FIGURE CAPTIONS

Figure 1. Relative transition probabilities for formation of specific product channels for charge transfer (exchange) scattering at 8 eV center-of-mass energy from $O_2^+(v = 1) + O_2(v' = 0)$. Product channels associated with each area are denoted by (v, v'). Calculations by the coupled-channel method were performed at selected values of orbital angular momentum ℓ given by the symbol +. The connecting lines are drawn by spline interpolation.

Figure 2. Same as Figure 1, except for direct scattering.

Figure 3. Absolute values of direct transition probabilities as a function of ℓ out of (1,0) at 8 eV to several indicated inelastic channels. Calculated values are marked by +. The connecting lines are drawn by spline interpolation.

Figure 4. Same as Figure 3 except for charge exchange scattering.

Figure 5. Absolute values of the $O_2^+(v = 1) + O_2(v' = 0)$ elastic charge exchange transition probability as a function of ℓ (and b) for 8 and 36 eV. Calculated values are marked by +. The connecting lines are drawn by spline interpolation.

Figure 6. Same as Figure 3 except for 36 eV.

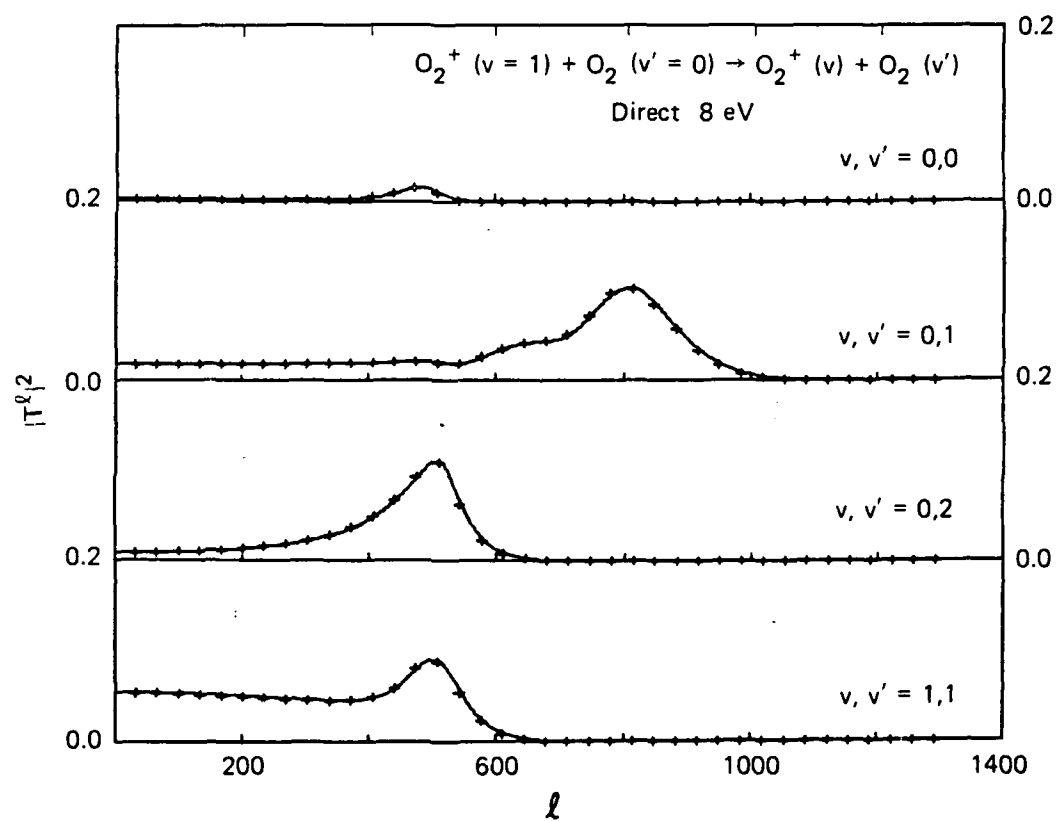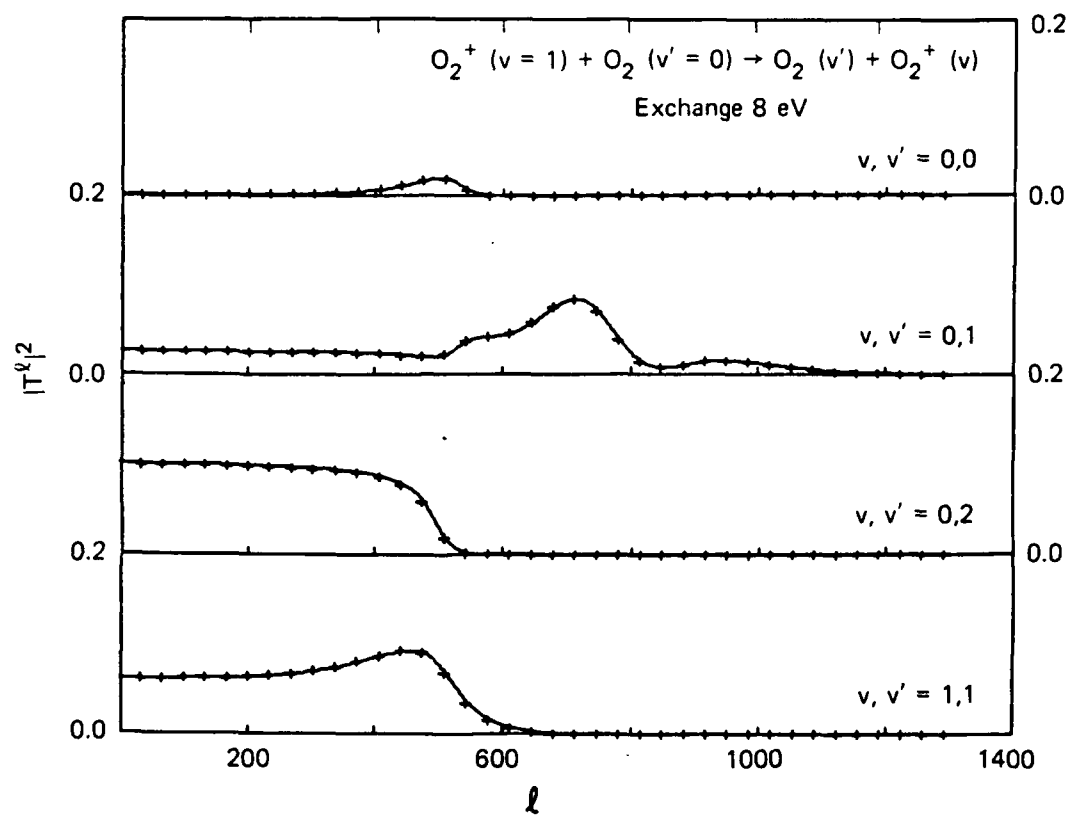Figure 7. Same as Figure 3 except for 36 eV and charge exchange scattering.

O$_2^+$ (v = 1) + O$_2$ (v = 0)
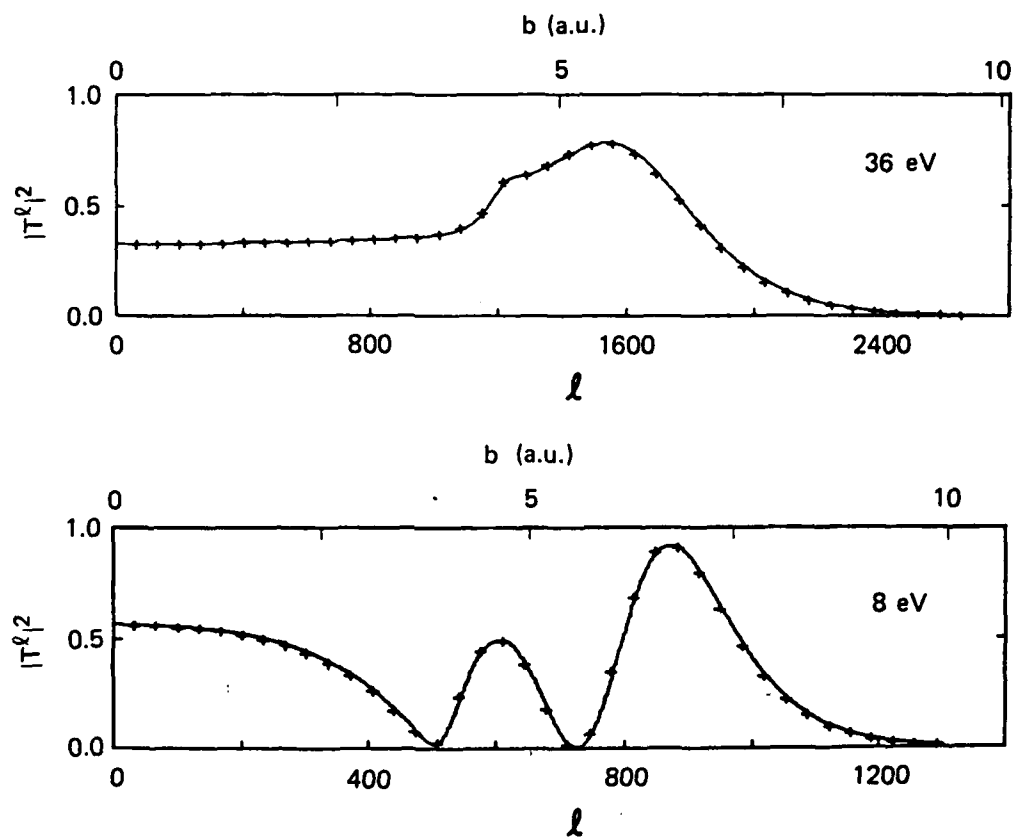EXCHANGE
8 eV

Fig. 1

C.H. Becker

$O_2{}^+ (v = 1) + O_2 (v = 0)$
DIRECT
8 eV

JA-1680-17B

Fig. 2

B-23

C.H. Becker

O_2^+ (v = 1) + O_2 (v' = 0) → O_2^+ (v) + O_2 (v')

Direct 8 eV

v, v' = 0,0

v, v' = 0,1

v, v' = 0,2

v, v' = 1,1

$|T^\ell|^2$

200   600   1000   1400

ℓ

JA-1680-22A

B-24

Fig. 3

C.H. Becker

$$O_2^+ \ (v = 1) + O_2 \ (v' = 0) \rightarrow O_2 \ (v') + O_2^+ \ (v)$$

Exchange 8 eV

$|T^\ell|^2$

ℓ

JA-1680-21A

Fig. 4
C.H. Becker

$$O_2^+ (v = 1) + O_2 (v' = 0) \rightarrow O_2 (v' = 0) + O_2^+ (v = 1)$$

Charge Exchange

Fig. 5 ??

C.H. Becker

$$O_2^+ (v = 1) + O_2 (v' = 0) \rightarrow O_2^+ (v) + O_2 (v')$$

Direct 36 eV

v, v' = 0,0

v, v' = 0,1

v, v' = 0,2

v, v' = 1,1

v, v' = 2,0

$|T^\ell|^2$

ℓ

JA-1680-19A

Fig. 6 IX

B-27

C.H. Becker

$O_2^+ (v = 1) + O_2 (v' = 0) \rightarrow O_2 (v') + O_2^+ (v)$

Exchange 36 eV

$v, v' = 0,0$

$v, v' = 0,1$

$v, v' = 0,2$

$v, v' = 1,1$

$v, v' = 2,0$

$|T^\ell|^2$

ℓ

JA-1680-20A

Fig. 7

C.H. Becker